

Engineering Notes

Real-Time Flight Trajectory Optimization and Its Verification in Flight

Takeshi Tsuchiya,* Masahiro Miwa,[†] and Shinji Suzuki[‡]
University of Tokyo, Tokyo 113-8656, Japan
and

Kazuya Masui[§] and Hiroshi Tomita[§]
*Japan Aerospace Exploration Agency,
Tokyo 181-8522, Japan*

DOI: 10.2514/1.41709

I. Introduction

THIS Note presents a real-time flight trajectory optimization method. The flight trajectory that minimizes the fuel consumption or flight time of an aircraft can be solved with optimization. Because the optimization is time-consuming, the optimal flight trajectory needs to be obtained before flight. This, however, cannot cope with unexpected situations in flight. Thus, the real-time optimization, which optimizes the flight trajectory with the transition of the flight state, is important. The final goal of our study is to establish the real-time trajectory generation applicable to emergency landing approaches. Though the present flight management system provides the optimal flight path for a flight plan in normal operations, it cannot operate in emergency situations. This Note presents a fundamental real-time trajectory optimization algorithm and its flight validation.

Many studies about real-time flight-path generation have produced a flight path by connecting the trim conditions in prestored databases [1,2]. In these studies, computer-assisted simulations were performed, but there were few actual flight experiments. Additionally, it is difficult to generate nonstational trajectories and the wind effects were not considered. In Japan, the Society of Japanese Aerospace Companies has promoted research on the development of a fault-tolerant flight control system. In a proceeding study, Suzuki et al. proposed a flight trajectory search method composed of a real-time A* algorithm and a random tabu search method [3]. They also conducted flight experiments. This random-based method, however, lacks convergent stability, so it often does not produce the appropriate trajectory.

We have taken over this study, and in this Note we apply a direct collocation method including some schemes to solve the preceding problems. Actual flight experiments are also conducted to prove the effectiveness of the method. The experimental aircraft is MuPAL- α , the Multi-Purpose Aviation Laboratory, developed by JAXA (Japan Aerospace Exploration Agency) [4]. It has a high-precision Global

Positioning System/inertial navigation system and a three-axis air-speed sensor. The system allows the estimation of the wind velocity and direction during flight. MuPAL- α also has a tunnel-in-the-sky display, which was developed by JAXA [5]. The experiments were conducted under manual tracking control using the display. In the future, the trajectory generated by the real-time optimization method will be tracked by an automatic flight control system being developed in the research on the fault-tolerant flight control system.

II. Definition of Flight Trajectory Optimization

A three-dimensional point-mass model is used to show the motion of the experimental aircraft MuPAL- α . The values of all the state variables, including the location and airspeed, are known at the present time ($t = t_{\text{present}}$) and the final time ($t = t_{\text{final}}$) when the optimal flight is finished, but the final time t_{final} is unknown. The aerodynamic characteristics are given as functions of angle of attack. Moreover, the state and control variables have upper and lower limits, as shown in Table 1. Because the pilot follows the optimal trajectory in this study, the limits are set from flight safety as well as the physical possibility.

A performance index function J minimized in this Note is mainly the flight time ($t_{\text{final}} - t_{\text{present}}$). A penalty function defined from the square integration of the differential values of the flight-path angle γ and bank angle ϕ is also included to generate smooth trajectories and reduce the pilot workload. The performance index is determined as follows:

$$J = t_{\text{final}} - t_{\text{present}} + \int_{t_{\text{present}}}^{t_{\text{final}}} (w_1 \dot{\gamma}^2 + w_2 \dot{\phi}^2) dt \quad (1)$$

Here, w_1 and w_2 are weight factors. The two variables γ and ϕ and their weight factor values are decided from flight simulator experiments.

III. Real-Time Flight Trajectory Optimization Method

The trajectory optimization method uses the BDH (block-diagonal Hessian) method [6]. This method discretizes all of the variables, motion equations, and constraint condition equations and transforms the trajectory optimization problem into a nonlinear programming problem. The optimal solution of the nonlinear programming problem is computed using a dedicated sparse sequential quadratic programming method.

A precondition for real-time flight trajectory optimization is that the overall trajectory from the present condition to the final condition is always obtained. The pilot wants to check the overall trajectory with the instrument display while flying. To optimize the overall trajectory at high speed, we add the following two schemes to the optimization method:

1) The optimization does not strictly pursue the transition of the flight state, but a position a little ahead of the current flight state is set as the initial condition.

2) If the overall optimal trajectory is computed, the optimization requires a lot of computation time when the aircraft flies far away from the final condition. This is because a long flight time requires many nodal points and many optimization variables.

Thus, the trajectory is divided into two intervals called stages, and dense nodal points are collocated to the interval nearest to the present position. The closer the trajectory, the more precise the trajectory obtained.

The following explains the real-time optimization algorithm based on the schemes (Fig. 1).

Received 19 October 2008; revision received 3 April 2009; accepted for publication 3 April 2009. Copyright © 2009 by the American Institute of Aeronautics and Astronautics, Inc. All rights reserved. Copies of this paper may be made for personal or internal use, on condition that the copier pay the \$10.00 per-copy fee to the Copyright Clearance Center, Inc., 222 Rosewood Drive, Danvers, MA 01923; include the code 0021-8669/09 and \$10.00 in correspondence with the CCC.

*Associate Professor, Department of Aeronautics and Astronautics; tsuchiya@mail.ecc.u-tokyo.ac.jp. Member AIAA.

[†]Graduate Student, Department of Aeronautics and Astronautics.

[‡]Professor, Department of Aeronautics and Astronautics. Senior Member AIAA.

[§]Senior Researcher, Flight Research Center, Aerospace Research and Development Directorate. Member AIAA.

Table 1 In-flight constraint conditions

Variable	Lower limit	Upper limit
Airspeed V	61.5 m/s	75.8 m/s
Flight-path angle γ	-5 deg	0.1 deg
Angle of attack α	-5 deg	15 deg
Bank angle ϕ	-15 deg	15 deg
Thrust T , N	$3440 - 51.8 \times V$, m/s	$20,800 - 129.5 \times V$, m/s

Step 1) Stage 0, of which the time length is T_{update} seconds, is defined. In stage 0, the aircraft flies in a steady horizontal flight. Although the aircraft flies in stage 0, the trajectory from the terminal condition of stage 0 to the final condition of the overall trajectory is optimized. Here, the T_{stage} second interval from the terminal state of stage 0 is defined as stage 1. The number of nodal points in stage 1 is N_1 , and the number of nodal points between the terminal state of stage 1 and the final condition is N_2 . The initial solution of the BDH method is set to the likely trajectory in which a level-turn straight-line descent or ascent and a level-turn flight appear one by one. The velocity in the initial solution changes at a constant rate during the straight-line descent or ascent flight. The optimization is stopped either when the solution converges near the optimal solution or the calculation time reaches T_{update} seconds and the trajectory is displayed on the instrument.

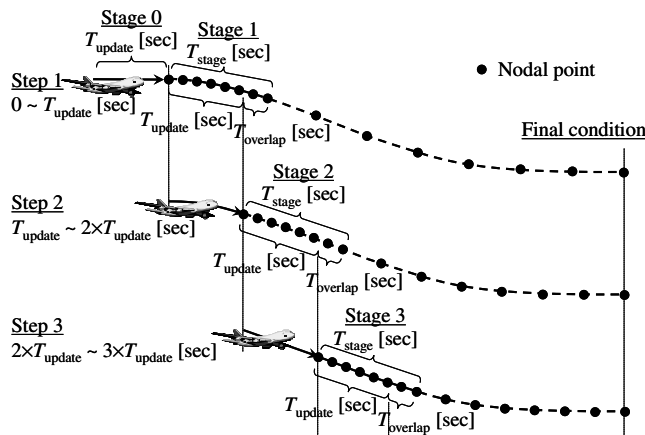
Step 2) Entering stage 1, the aircraft starts to fly along the trajectory obtained in step 1. Although the aircraft flies within the first T_{update} seconds in stage 1, the trajectory roughly optimized in the previous step is reoptimized with higher accuracy. Stage 2 is defined as a T_{stage} second interval of which the initial state is the state at T_{update} seconds in stage 1. Here, because the trajectories are connected smoothly, stage 2 overlaps the last T_{overlap} seconds of stage 1. The numbers of nodal points in stage 2 and in the other interval are N_1 and N_2 , respectively. The optimal trajectory obtained in step 1 can be used as the initial solution in this step. Before the T_{update} second flight in stage 1, the optimization is stopped.

Step 3) The aforementioned process is repeated until the aircraft gets close to the final condition. If the remaining flight time to the final condition is within T_{terminal} seconds, the overall trajectory is discretized with $N_1 + N_2$ nodal points and optimized at once.

In the optimization, we should consider wind effects; otherwise, it is very difficult for pilots to follow the optimized trajectory. The average wind velocity and direction, which can be measured by MuPAL- α , are calculated in one step and incorporated in the next step. The optimization parameters, which were decided based on the computer power, are summarized in Table 2. We used a personal computer with an Intel Core 2 Duo T7600 (2.33 GHz) CPU.

IV. Numerical Simulations

We compared the real-time optimization with an offline optimization to confirm the effectiveness of the real-time flight trajectory

**Fig. 1 Real-time optimization algorithm.****Table 2 Parameters of real-time optimization**

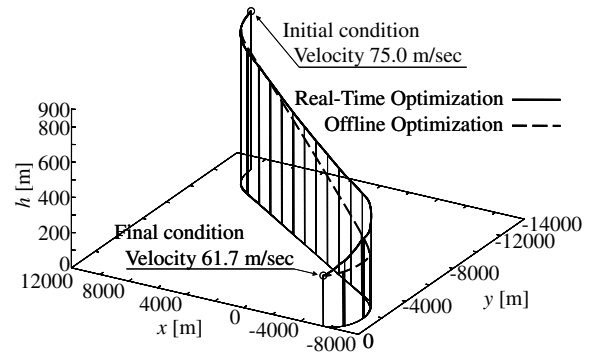
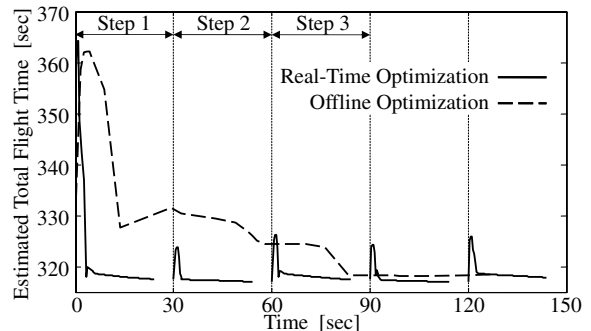
Parameter	Value
N_1	40
N_2	40
T_{stage}	40 s
T_{update}	30 s
T_{overlap}	10 s
T_{terminal}	90 s

optimization. The offline optimization optimizes the entire trajectory at once. The interval of the nodal points in the offline optimization is almost equal to that of the nearest stage in the real-time optimization. The values of the weight factors w_1 and w_2 in Eq. (1) are zeros in this section.

Figure 2 shows the flight trajectories of the real-time optimization and offline optimization. The figure omits stage 0 of the real-time optimization trajectory. The total flight times of the real-time optimization and offline optimization are 320.0 and 318.4 s, respectively; both are almost equal. The horizontal projection of the trajectory, airspeed history, bank-angle history, and angle-of-attack history of the real-time optimization almost correspond to those of the offline optimization, but the flight-path angle of the real-time optimization oscillates to satisfy the final conditions. The oscillation can be suppressed by the weight factors w_1 and w_2 . Figure 3 shows the convergence histories of the estimated total flight time. Though the offline optimization takes more than 90 s for convergence, the real-time optimization converges sufficiently within T_{update} seconds in each step.

V. Actual Flight Experiment

The actual flight experiments were performed to confirm whether the proposed real-time optimization worked well and pilots could track the trajectories in actual environmental conditions. In flight simulator experiments before the actual flight experiments, we

**Fig. 2 Comparison of flight trajectories.****Fig. 3 Comparison of convergence histories of performance functions (estimated total flight times).**

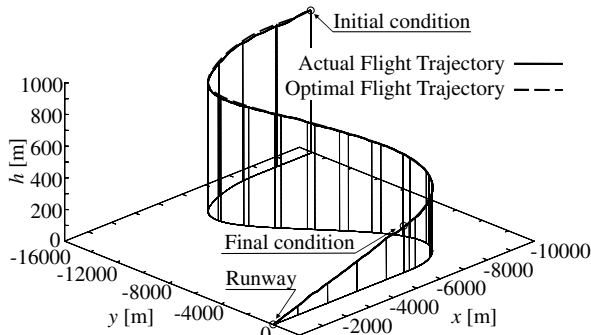


Fig. 4 Flight trajectories in case 1.

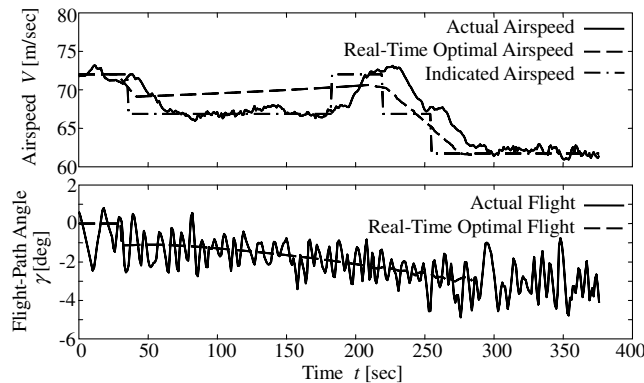


Fig. 5 State variable histories in case 1.

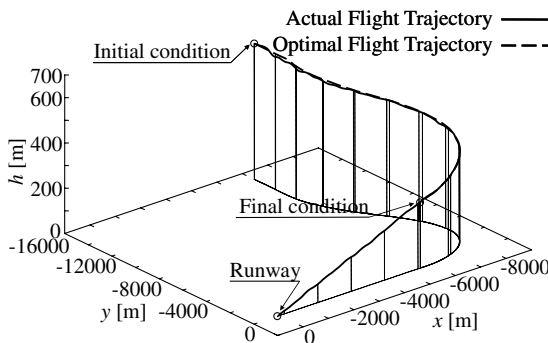


Fig. 6 Flight trajectories in case 2.

decided the weight factors, $w_1 = 1.0 \text{ s}^2$ and $w_2 = 0.01 \text{ s}^2$, with which we could confirm the effectiveness of the optimization without giving the pilots a heavy workload. This Note shows two of the flights. The flights assumed landing approaches near a runway. At the final conditions, the trajectories were connected to glide paths for the runway. Figures 4–7 show the flight results until the runway. The figures of the airspeed histories also include the commands indicated to the pilots. Displaying the optimal airspeed accurately gave the pilots a heavy workload for throttle adjustment. Thus, we displayed the target airspeed at 10 kt intervals. The wind velocity observed during the flight experiments was from 5 to 20 kt, and about 10 kt on average. Though the flight-path angle, angle of attack, and bank angle of the actual trajectories oscillate due to the shifting flight environment, such as wind disturbance, all the states satisfy the constraint conditions. The proposed real-time optimization worked

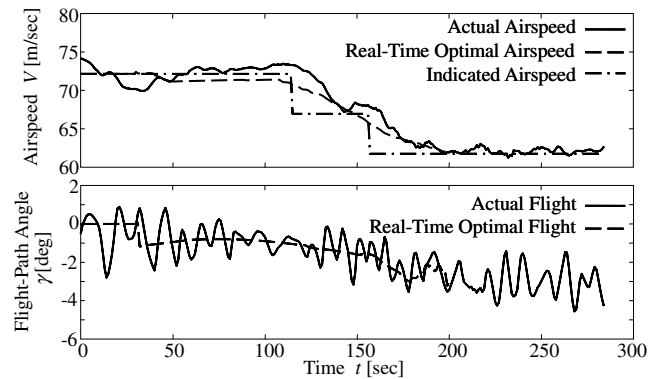


Fig. 7 State variable histories in case 2.

well even in the actual flight experiments, and the pilots were adequately able to follow the optimal flight trajectories.

VI. Conclusions

This study developed the real-time flight trajectory optimization method. A feature of the optimization method is that the forthcoming condition on the already-obtained overall trajectory was defined as the initial condition and the optimization was recalculated by the time the aircraft reached the initial condition. In addition, the nodal points of the trajectory optimization method were well allocated to achieve a good balance between the optimization speed and precision. In the numerical simulation, the real-time optimization showed good convergence characteristics and could produce the trajectory that was almost equal to the optimal trajectory of the offline optimization. In addition, the actual flight experiments were performed with manual tracking of pilots. The pilots could track the optimal flight trajectories with good accuracy. In the future, we will conduct more simulations and flight experiments under various situations and integrate the real-time optimization method in an automatic flight control system.

Acknowledgments

This research program was funded by the Ministry of Economy, Trade, and Industry and was organized by the Society of Japanese Aerospace Companies.

References

- [1] Valenti, M., Mettler, B., Schouwenaars, T., Feron, E., and Paduano, J., "Trajectory Reconfiguration for an Unmanned Aircraft," AIAA Guidance, Navigation, and Control Conference and Exhibit, Monterey, CA, AIAA Paper 2002-4674, 2002.
- [2] Atkins, E., Portillo, I., and Strube, M., "Emergency Flight Planning Applied to Total Loss of Thrust," *Journal of Aircraft*, Vol. 43, No. 4, 2006, pp. 1205–1216.
doi:10.2514/1.18816
- [3] Suzuki, S., Komatsu, Y., Yonezawa, S., Masui, K., and Tomita, H., "Online Four-Dimensional Flight Trajectory Search and Its Flight Testing," AIAA Guidance, Navigation, and Control Conference and Exhibit, San Francisco, AIAA Paper 2005-6475, 2005.
- [4] Masui, K., and Tsukano, Y., "Development of a New In-Flight Simulator MuPAL- α ," AIAA Modeling and Simulation Technologies Conference, Denver, CO, AIAA Paper 2000-4574, 2000.
- [5] Funabiki, K., Muraoka, K., Terui, Y., Harigae, M., and Ono, T., "In-flight Evaluation of Tunnel in the Sky Display and Curved Approach Pattern," AIAA Guidance, Navigation, and Control Conference and Exhibit, Portland, OR, AIAA Paper 1999-3966, 1999.
- [6] Yokoyama, N., Suzuki, S., and Tsuchiya, T., "Convergence Acceleration of Direct Trajectory Optimization Using Novel Hessian Calculation Methods," *Journal of Optimization Theory and Applications*, Vol. 136, No. 3, 2008, pp. 297–319.
doi:10.1007/s10957-008-9351-0